RNA BIOLOGY
2017, VOL. 14, NO. 1, 29–35
http://dx.doi.org/10.1080/15476286.2016.1256532

Taylor & Francis
Taylor & Francis Group

BRIEF COMMUNICATION

OPEN ACCESS

Characterization of genetic loss-of-function of Fus in zebrafish

Svetlana Lebedeva, António M. de Jesus Domingues, Falk Butter, and René F. Ketting

Institute of Molecular Biology, Mainz, Germany

ABSTRACT
The RNA-binding protein FUS is implicated in transcription, alternative splicing of neuronal genes and DNA repair. Mutations in FUS have been linked to human neurodegenerative diseases such as ALS (amyotrophic lateral sclerosis). We genetically disrupted *fus* in zebrafish (*Danio rerio*) using the CRISPR-Cas9 system. The *fus* knockout animals are fertile and did not show any distinctive phenotype. Mutation of *fus* induces mild changes in gene expression on the transcriptome and proteome level in the adult brain. We observed a significant influence of genetic background on gene expression and 3′UTR usage, which could mask the effects of loss of Fus. Unlike published *fus* morphants, maternal zygotic *fus* mutants do not show motoneuronal degeneration and exhibit normal locomotor activity.

Abbreviations: ALS, amyotrophic lateral sclerosis; NLS, nuclear localization sequence; FET, Fus; Taf15, Ewsr1 family of RNA-binding proteins; LC domain, low complexity domain; CTD, C-terminal domain (of RNA polymerase II); GO, gene ontology; hpf, hours post fertilization; dpf, days post fertilization; MZ, maternal zygotic; MO, morpholino

ARTICLE HISTORY
Received 15 August 2016
Revised 24 October 2016
Accepted 30 October 2016

KEYWORDS
CRISPR-Cas9; Danio rerio; Fus; genetic knockout; morpholino; zebrafish

Introduction

RNA-binding proteins that carry aggregation-prone prion-like domains have recently gained attention due to their involvement in many cellular processes and disease.[1] One of the most studied of these proteins is FUS ("Fusion," or TLS, "translocated in liposarcoma"). FUS belongs to a conserved family of RNA-binding proteins (FET family, from the names of the members FUS, EWSR1, and TAF15) which shuttle between the nucleus and cytoplasm, are predominantly nuclear in steady-state and have long N-terminal domains of low complexity (Q, S,G,Y-rich stretches, further called LC domains). In addition, they contain RGG motifs, one RRM and one RanBP2-type Zinc finger domain.[2] FUS plays roles in regulation of splicing, especially co-transcriptional splicing of long neuronal pre-mRNAs,[3-7] 3′end definition of mRNAs,[8] DNA repair and the formation of nuclear foci: paraspeckles[9] and Gems.[10] The LC domain provides FUS with the ability of phase transition, enabling it to form RNP foci.[11] Mutations in the FUS nuclear localization sequence (NLS) which are associated with the disease ALS (amyotrophic lateral sclerosis) lead to FUS depletion from the nucleus and its aggregation in the cytoplasm of motoneurons, and eventually to motoneuronal death.[12,13] While both the loss of function of FUS in the nucleus, and toxicity of the cytoplasmic FUS aggregates can contribute to neurodegeneration, most recent data suggest that a gain of function of FUS is detrimental.[14,15] Several independently produced rodent models show ALS-like neurodegeneration phenotypes upon overexpression of wild-type FUS,[16,17] while the loss-of-function of FUS alone produces phenotypes different from ALS in mice.[18-20] Zebrafish injected with antisense morpholino oligonucleotides against *fus*, as well as overexpressing mutant *fus* mRNA display motoneuron degeneration and swimming defects.[21-23] Given recent controversies in the field regarding the non-specific effects of morpholinos and the readily available CRISPR-Cas9 technique we created a genetic knockout zebrafish model to study *fus* loss-of-function. We show that contrary to morpholino, and similar to mouse *Fus* knockout, genetic loss-of-function of Fus does not cause an ALS-like phenotype in zebrafish. We also report high-throughput transcriptomic and proteomic profiling of the adult zebrafish *fus* knockout brain.

Results

Fus *knockout alleles in zebrafish*

We used CRISPR-Cas9 technology[24] to disrupt the zebrafish *fus* gene with a single guide RNA targeting exon 3 (Fig. 1A). All subsequent analyses were performed on the allele that deletes 8 base pairs, resulting in a frameshift and a premature stop codon ("Δ8" allele) (Fig. 1A, B). The Δ8 *fus* mRNA was still present in knockout animals, although it was approximately 2 times less abundant than the wt mRNA (Fig. 1C). The published antibodies used to detect zebrafish Fus protein on Western blot[21] failed to detect Fus in wild type embryos in our hands (not shown). Therefore we used mass spectrometry (MS) in order to determine if the Δ8 *fus* mRNA was still able to produce protein. To minimize a possible contribution of maternally deposited protein, we analyzed 5 day-old embryos from a heterozygous

CONTACT René F. Ketting r.ketting@imb.de
Supplemental data for this article can be accessed on the publisher's website.
Published with license by Taylor & Francis Group, LLC. © Svetlana Lebedeva, António M. de Jesus Domingues, Falk Butter, and René F. Ketting
This is an Open Access article distributed under the terms of the Creative Commons Attribution-Non-Commercial License (http://creativecommons.org/licenses/by-nc/3.0/), which permits unrestricted non-commercial use, distribution, and reproduction in any medium, provided the original work is properly cited. The moral rights of the named author(s) have been asserted.

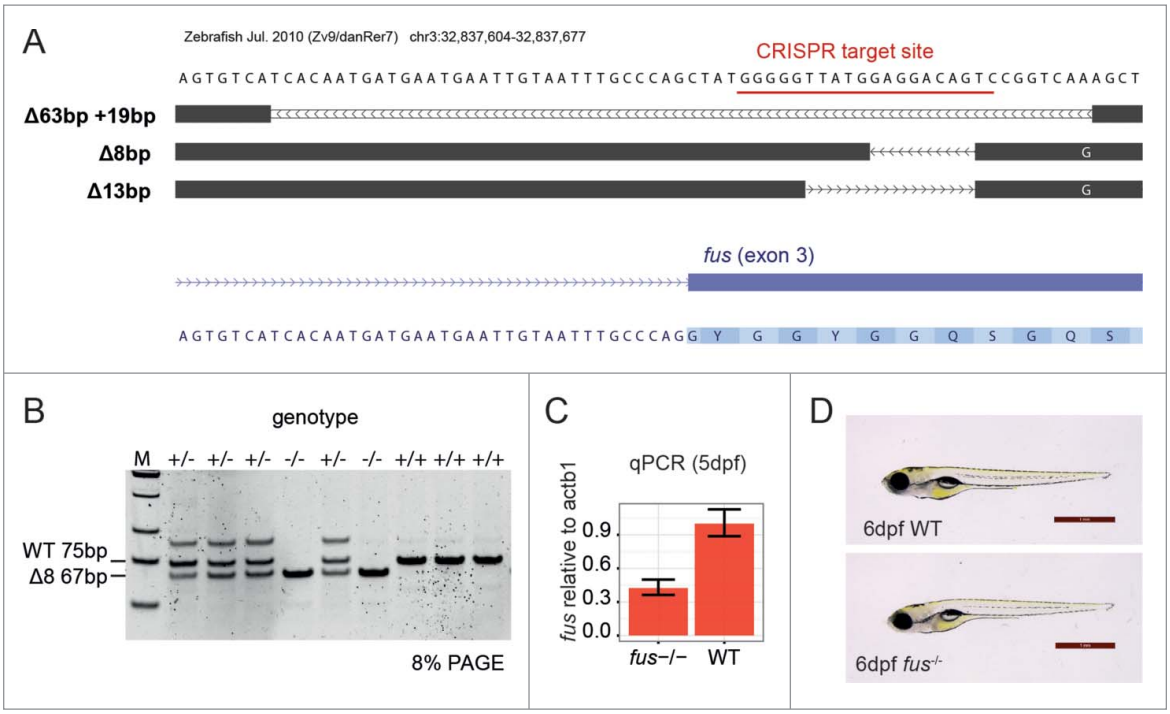

Figure 1. Generation and validation of the *fus* knockout zebrafish. (A) *fus* alleles generated by CRISPR-Cas9. A screenshot from the UCSC genome browser shows aligned sequences from heterozygous F1 animals. CRISPR target site in *fus* exon 3 is underlined in red. (B) An example of a PAGE gel for genotyping the Δ8 allele. M = Low molecular weight marker. Wild type (75bp) and $fus^{-/-}$ (67bp) products can be discriminated. (C) Quantification of *fus* mRNA relative to WT mRNA in 5dpf embryos. (D) Normal morphology of the WT and $fus^{-/-}$ embryo at 6 d post fertilization (dpf). Scale bar is 1mm.

incross. No peptides unique to Fus protein were detected in any of the 4 replicates of $fus^{-/-}$ embryos, whereas 2 Fus-unique peptides were present in $^3/_4$ replicates of the wild type siblings (Table 1). This analysis led us to conclude that Fus protein was not produced and the *fus* Δ8 allele is a loss-of-function mutation.

Transcriptome and proteome analysis of fus *knockout brain*

Fus homozygous knockout fish, including maternal zygotic mutants, are viable, fertile and appear morphologically normal (Fig. 1D). In search for molecular consequences of loss of Fus, we performed gene expression analysis on adult brains of $fus^{-/-}$ animals and wild type siblings. Fus is ubiquitously expressed with the highest expression found in brain, as shown by *in situ* hybridization and qPCR (Fig. S1A, B),[21] immunostaining[21] and as inferred from publicly available RNA-Seq data.[25] Also, numerous splicing changes have been reported for FUS loss-of-function in the mouse brain and spinal cord.[3-5,15] We therefore considered brain to be the most relevant tissue to search for gene deregulation upon loss of Fus. We performed paired-end sequencing of the polyA+ transcriptome from brains of 5 $fus^{-/-}$ and 4 wild type animals (Fig. 2A). All animals were 8-month old female siblings. The most significantly changed gene was *fus* itself, and only 5 other transcripts changed over 2-fold (Fig. 2B and Table S1). We selected 16 genes and validated their fold changes with qPCR using independently dissected brains (Fig. S1C). Changes in alternative splicing are a hallmark of the FUS-dependent regulation in mouse brain. However, in the zebrafish $fus^{-/-}$ brain we did not reliably identify strong changes in alternative splicing using

Table 1. Identification of Fus by mass-spectrometry (MS). Peptides unique to Fus protein were only identified in the MS analysis of the WT 5dpf embryos and adult brain, but not in the Fus knockout. Cross (x) signifies that the peptide was identified in the respective sample. Below: Fus full protein sequence, detected peptides unique for Fus are bold and underlined.

		wild type				$fus^{-/-}$			
Sample	Sequence	repl. 1	repl. 2	repl. 3	repl. 4	repl. 1	repl. 2	repl. 3	repl. 4
Embryo	AAIDWFDGKDFNGNPIK	X							
	TGLPMINLYTDR		X		X				
Brain	AAIDWFDGKDFNGNPIK	X	X	X	X				
	CSNPSCGNLNFSWR	X	X	X					
	TGLPMINLYTDR	X							

MASNDYGQTSSHGYGGYGGQSGQSYSQPSAQNYSQQSYGGYNQSSESSSAPYNQGGYSSNYGQSQSGGYGSQAPSQGYSQSSQSYSSGGYSNTSQPPPAQSGGYSQQSSYSGYNQSSPASAP
GGYSSSSQSSGYGQQQQQSGGGYGGSGGQSGGYGSSGGQSSGFGGSGGQHQSSQSGGGSYSPSPNYSSPPPQSYGQQSQYGQGGYNQDSPPMSGGGGGGGYGGQDGGYSQDGRGGRG
RGGGFGGRGAGGFDRGGRGGPRGRGGMGMGDRGGFNKFGGPRDHGAGGPNMQEQDNSDNNTIFVQGLGDDYTVDSVADYFKQIGIIKVNKK**TGLPMINLYTDR**ETGKLKGEATVSFDDPP
SAK**AAIDWFDGKDFNGNPIK**VSFATRRAEFGRGGSSGGMRGGRGRGGPMGRGGFGGGRGGGGGGGGFQGNNGGGSGNGGGQQRAGDWK**CSNPSCGNLNFSWR**NECNQCKEPKPEGSG
GGMSPMGGGFGGERGRSGFDRGGFRGRGGDRGGFRGGRGGDRGGFGPGKMDSRGDHRHDRRDRPY

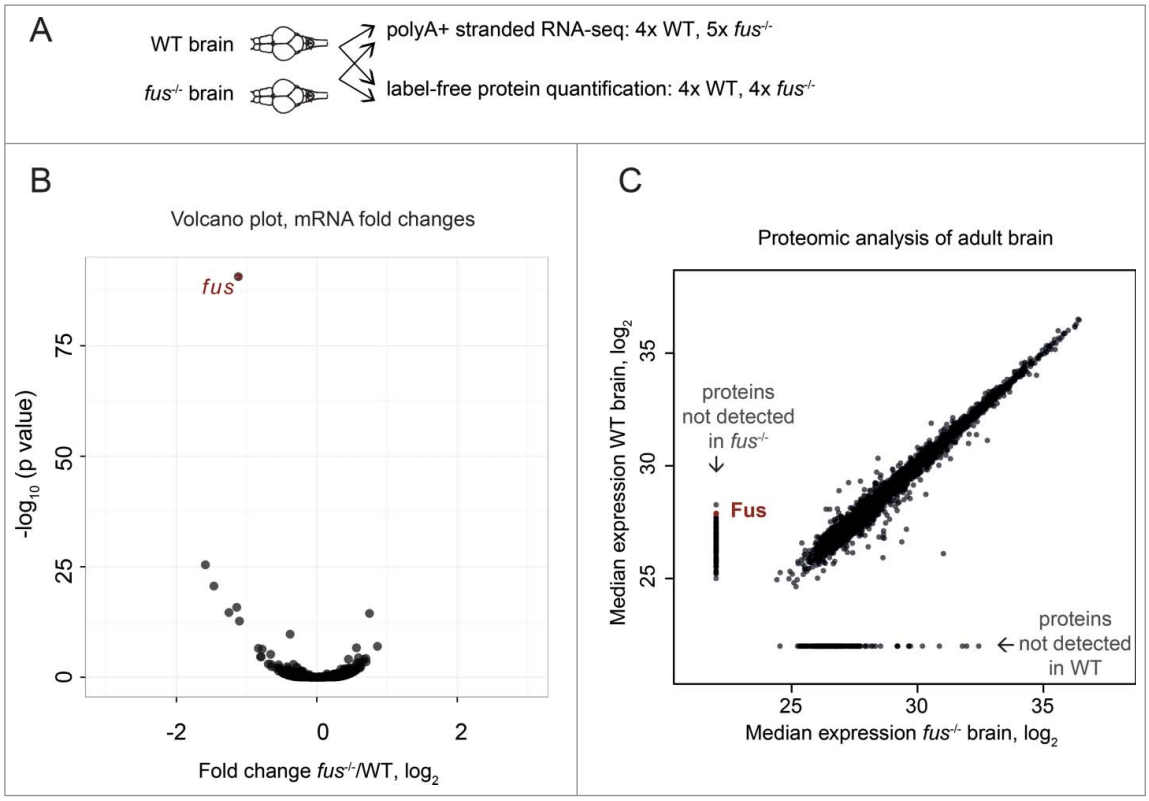

Figure 2. Transcriptome and proteome of the *fus*$^{-/-}$ brain. (A) Adult. zebrafish brains from either *fus*$^{-/-}$ or WT siblings were used to simultaneously quantify mRNAs by RNA sequencing and proteins by mass-spectrometry. In total, transcriptomes of 5 *fus*$^{-/-}$ and 4 WT, and proteomes of 4 *fus*$^{-/-}$ and 4 WT animals were measured. (B) Volcano plot of mRNA fold changes displays the fold change (on the x axis) and p-value (on the y axis). *fus* is the most significantly changed gene on mRNA level (labeled in red) (C) Quantification of the proteome by label-free mass-spectrometry. Label-free quantification was performed as previously described.[43] Median expression of the proteins in WT brain (y axis) is plotted against the expression in *fus*$^{-/-}$ brain (x axis) on the log scale. Proteins not detected in one of the samples were assigned an arbitrary value of 22. Fus is among the highest expressed proteins that were detected in WT and missing from the knockout (marked in red).

several available tools (DEXSeq, MISO, cuffdiff, data not shown). Likewise, identified FUS targets with long introns reported to be downregulated in FUS knockdown mouse brain[3] failed to show comparable changes in zebrafish (Fig. S2). In parallel to the transcriptome analysis, we quantified proteins using 4 replicates of the RNA-profiled brain lysates using label-free quantitative mass spectrometry. In accordance with the transcriptome, protein steady-state levels remained unchanged upon loss of Fus (Fig. 2C and Table S2).

Genetic background affects alternative 3′UTR usage

During analysis of the RNA-sequencing data, we noticed that some genes display large variation in gene expression among siblings (biological replicates), independent of the *fus* genotype (Fig. S3). Zebrafish cannot be maintained as inbred lines because of inbreeding depression,[26] and the background of our line is mixed (AB × TU). We reasoned that genetic background effects may prevail over subtle effects of *fus* knockout. To address this issue more systematically, we chose to focus on alternative polyadenylation site usage, which is relatively straightforward to quantify and visualize. We used isoSCM[27] to *de novo* detect 3′UTR isoforms, and quantified their differential expression. Next, we called single nucleotide polymorphisms (SNPs) from the RNA-Seq data taking advantage of the sufficient read coverage over the 3′UTRs. Indeed, the top differential 3′UTRs isoforms often followed the distribution of SNPs, and not the *fus* genotype (Fig. 3). Thus, we are able to detect differential isoform expression in our RNA-Seq data, but the isoform usage seems to be more strongly influenced by local genetic background than by the expression of Fus.

Fus *knockout embryos lack motoneuronal defects*

It has been previously reported that zebrafish *fus* morphants display defects in motoneurons.[21,22] These defects comprise severe shortening of motoneuronal axons and their excessive branching, abnormal formation of neuromuscular junctions and impaired locomotion. We asked if some of these defects could be observed in maternal zygotic *fus* knockout (MZ*fus*$^{-/-}$) embryos. To address the structure of primary motoneuronal axons we crossed *fus* mutants to the Nbt:dsRed reporter line expressing DsRed fluorescent protein under the control of neuronal specific promoter (*Xenopus* neural-specific β tubulin promoter).[28] We imaged transgenic embryos at the age of 36 hours post fertilization (hpf) (Fig. 4A). We did not observe shortening of motoneuronal axons in both zygotic and maternal zygotic *fus*$^{-/-}$ embryos compared with wild type siblings (n = 5 wild type, 6 zygotic and 7 maternal zygotic *fus*$^{-/-}$ embryos). More detailed, quantitative analysis also did not reveal strong differences in branching between wt and mutant axons (Fig. S6). We further assessed motor activity of *fus*$^{-/-}$ embryos by performing the touch-evoked escape response assay.[29] In this assay, 2 day old embryos are placed in the middle of a dish with embryonic medium and the tail is slightly touched

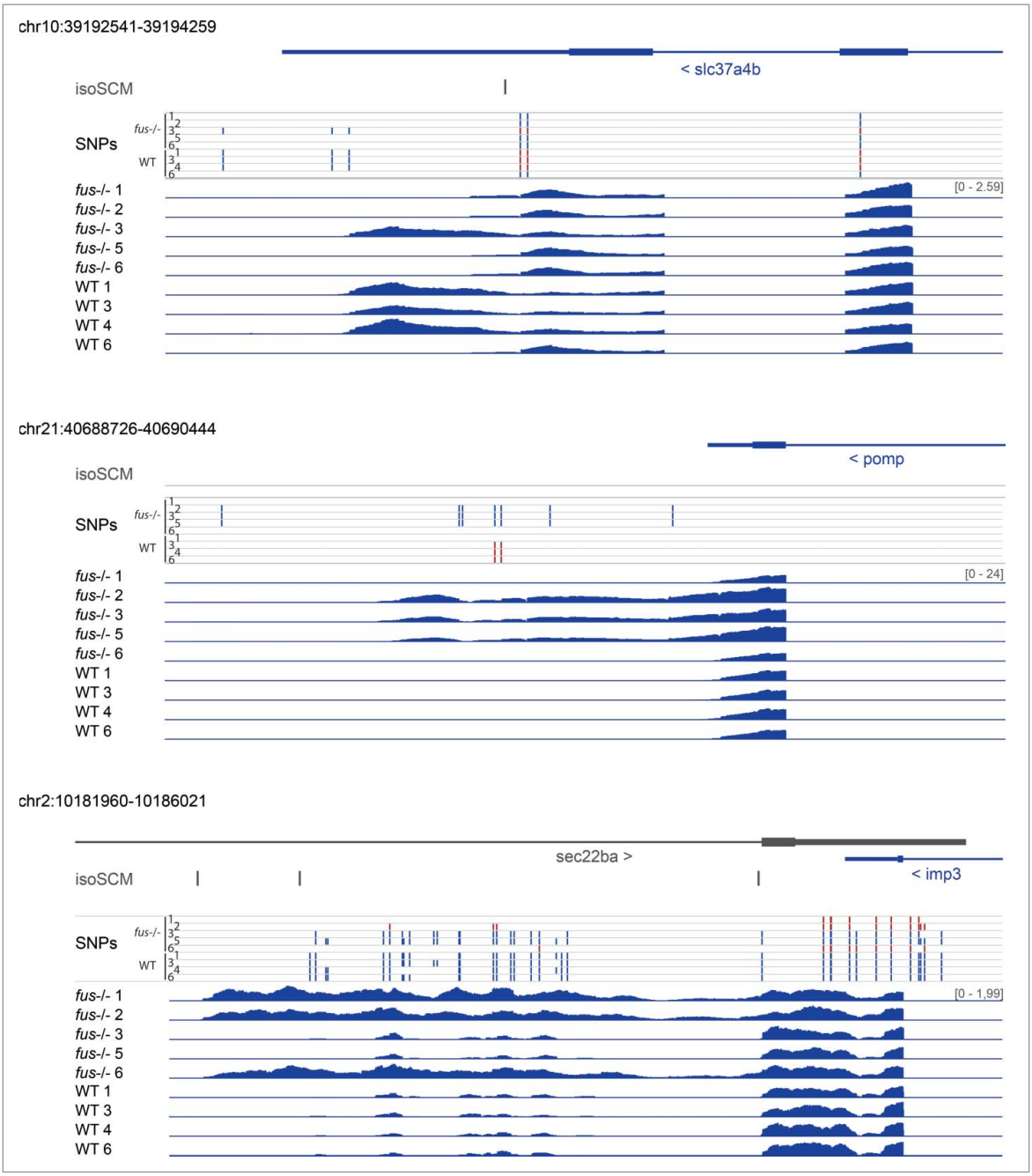

Figure 3. Examples of alternative 3′UTR usage in different genetic backgrounds. Shown are screenshots from IGV genome browser. The relevant genes are *slc37a4b, pomp* and *imp3*. For convenience, RNA-Seq coverage tracks are shown in blue only for the minus strand. Called SNPs that have been filtered (see methods) are represented by colored bars above the gene track. Dark blue are homozygous variants, dark red bars are heterozygous; homozygous reference or absent calls are not shown. The isoSCM track shows putative alternative 3′ends called by isoSCM. The scale for RNA-Seq coverage is normalized to 1,000,000/(total read count) and is the same for all tracks (shown in gray in square brackets on the right).

with forceps. Healthy embryos respond to the touch by swimming away (escaping). Embryos with motoneuron impairment are expected to swim a shorter distance. We quantified the length of the swim tracks and did not find a significant difference between wild type and *fus*$^{-/-}$ embryos (Fig. 4B). Since we could not see the locomotor phenotype upon loss of Fus, we tried to reproduce the published *fus* morpholino experiments[21,22] using the same line (AB × TU) in which the *fus* mutant was generated. Surprisingly, we could not detect a significant reduction in swim distance for the *fus* morpholino injected embryos (Fig. S4A, left panel), even though we confirmed that the *fus* morpholino was functional by co-injecting GFP mRNA carrying the *fus* morpholino target site (Fig. S4B). We reasoned that our outbred strain might have a different response to morpholino injection. We therefore performed the touch response assay on *fus* MO-injected fish with an AB background and observed a trend for reduced swim distance in MO-injected, but not in control MO-injected embryos. Nevertheless, the difference was still not significant ($p = 0.103$) (Fig. S4A, right panel).

Discussion

We report the generation of a *fus* knockout zebrafish model and its phenotypic characterization. Maternal zygotic *fus* knockouts are

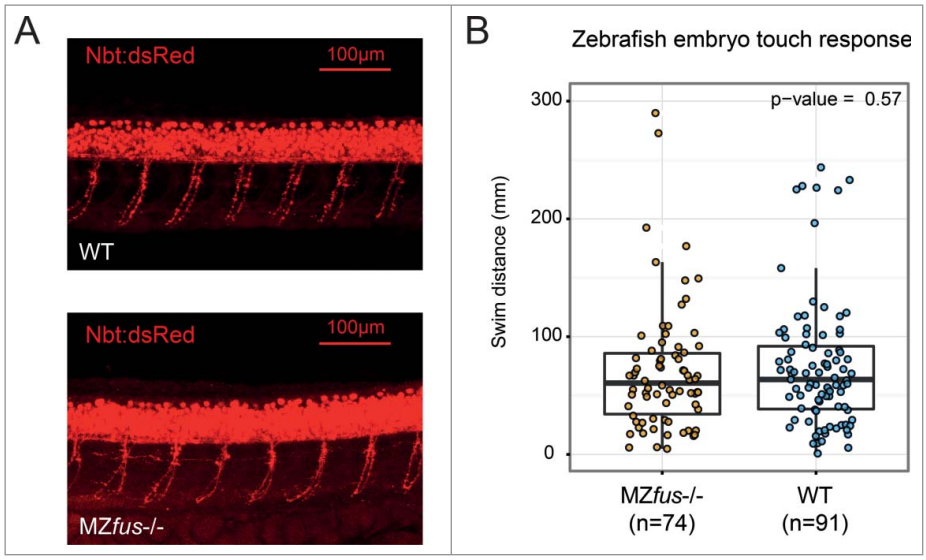

Figure 4. Motoneuron morphology and touch evoked escape response of *fus* knockout larvae. (A) Confocal images of trunks of 36hpf larvae expressing neuron-specific DsRed.[28] Maternal zygotic Fus knockout larvae show normal overall primary motoneuron axon morphology indistinguishable from WT. Maximal intensity projection of a confocal stack is shown; scale bar is 100μm. (B) Touch evoked escape response of 2dpf (48–52hpf) larvae. Swim distances in mm for individual larvae tracks are plotted. P-value is from Kruskal-Wallis test. n indicates the number of larvae tested for each group.

healthy and fertile. In contrast to one of the mouse knockouts,[19] *fus* knockout zebrafish are not radiation sensitive (data not shown). The brain transcriptome and proteome was only slightly affected by the loss of Fus protein, with most changes being less than 2-fold. This is in line with the most recent RNA-Seq data from the mouse FUS knockout brain where only ~10% of the changes were more than 1.5-fold.[15] Overall, our results with Fus knockout zebrafish add to the idea that, in vertebrate model organisms, Fus loss-of-function alone does not elicit the neurodegenerative phenotype seen in FUS-related diseases, supporting recent mouse data.[18] It is tempting to speculate that other members of the FET family, Taf15 and Ewsr1, may compensate for the loss of Fus in vertebrates. *Drosophila*, which has only one homolog of FET proteins, Cabeza, does show reduced survival and impaired locomotion upon its inactivation,[30] and simultaneous depletion of FUS and TAF15 in human motoneurons results in gene expression profile similar to that in ALS patient-derived neurons bearing the ALS mutation FUS^{R521G}.[31] It is interesting to note as well that in zebrafish the genetic knockout of another ALS-related RNA-binding protein Tardbp apparently causes neurodegeneration followed by muscular atrophy, but only if its paralog Tardbpl is also inactivated.[32] FET proteins are similar in structure, localization, have partially overlapping targets[33] and interact with each other.[34] Notably, none of the FET proteins was upregulated in our Fus knockout (Fig. S1C), suggesting that genetic compensation does not take place. However, since zebrafish has 4 FET proteins as compare with 3 in all mammals, it is still plausible that upregulation is not necessary to compensate for the loss of Fus. Simultaneous knockout of several FET proteins in zebrafish may elicit stronger phenotype.

We used outbred zebrafish (AB × TU) to generate *fus* knockout animals. This strategy was beneficial, since embryos in TU background injected with highly concentrated Cas9 and guide RNA showed poor survival. However, we observed that the genetic background can strongly influence gene expression and alternative isoform usage. These effects could have obscured mild expression changes resulting from the loss of Fus. In addition, our data suggest that effects of morpholino injections can manifest differently depending on the genetic background of the embryos. In line with this, several FUS knockout mouse models show a wide spectrum of phenotypes which range from postnatal lethality in more inbred lines to surviving adults with mild morphological and behavioral defects in an outbred line.[18-20] Since the high density of SNPs, and outbred nature of zebrafish is more similar to that in humans than that in inbred mouse lines, zebrafish can represent a very useful model to study the effects of Fus, or that of any other protein, within the context of naturally occurring genetic variation.

Data

Raw RNAseq data are deposited in GEO (GSE85554). Proteomics data have been deposited to the ProteomeXchange Consortium via the PRIDE partner repository with the data set identifier PXD004876e.

Methods

Extended methods can be found in the Supplementary material.

Fish husbandry and strains

Fish were maintained, raised, and staged as described before.[35] Unless stated otherwise, in all experiments a mix of AB and TU strain was used. All experiments were performed according to German animal welfare law (licenses 23 177–07/G 13–5–087 (CRISPR-Cas9 knockouts), 23177–07/A 15–5–001 OES (tail fin clips)). CRISPR-Cas9 knockouts were generated as described.[24]

mRNA sequencing

Strand-specific polyadenylated RNA libraries were prepared using the TruSeq Stranded RNA Library Preparation Kit and

sequenced on an Illumina HiSeq2000 using the 2 × 100bp read protocol. RNA-sequencing reads were mapped to the zebrafish genome (Zv10) using the aligner STAR (version 2.4.1d[36]). Read count Table was produced with featureCounts (v. 1.4.6[37]) using Ensembl database gene annotation (release 80). Differentially expressed genes were called using R package DESeq2.[38]

Mass spectrometry

Mass spectrometry sample preparation and measurement was done as described[39] except a 50 cm C18 column and a 240 minute LC gradient was used. Samples were analyzed with MaxQuant (version 1.5.2.8[40]) against the supplied Uniprot zebrafish database (39,559 entries) with standard settings, except LFQ values were based on unique peptides. For data analysis, information about identified peptides was extracted from the evidence table. On the protein level, the median LFQ values were calculated for each condition (WT, *fus*$^{-/-}$) from the protein groups file and plotted as a scatterplot in R using the ggplot2 package.[41]

Confocal imaging

Zebrafish trunks were imaged on Leica SP5 confocal microscope. Maximal projection images were generated with Fiji software.[42]

Morpholino injections

Fus morpholino (GGCCATAATCATTTGACGCCATGTT)[21] and 5-mismatch control morpholino (GCCCATAATGATTT CACGGCATCTT) were from Genetools. Approximately 1nl drop of 1mM Fus morpholino was injected into 1-cell stage embryos.

Touch evoked response assay

Embryos at 2dpf were placed in a 15cm dish with embryonic medium, lightly touched with forceps at the tail, and movements were video recorded using a Basler acA2000–165um Monochrome USB camera with the speed of 40 frames per second. A ruler was placed next to the dish to calibrate the track lengths in mm. The videos were processed in Fiji[42] using a customized macro script and MTrack2 plugin (http://valelab.ucsf.edu/∼nstuurman/ijplugins/MTrack2.html). Only complete tracks were considered for statistical analysis.

Disclosure of potential conflicts of interest

No potential conflicts of interest were disclosed.

Acknowledgments

We kindly thank members of the IMB Genomics, Microscopy and Proteomics core facilities for technical assistance and reagents, especially Nastasja Krejm from the IMB Bioinformatics core facility for the initial data analysis and Sandra Ritz from Microscopy core facility for help with imaging and analysis of motoneurons, Natalie Schützler and Veronika Prantl from the Johannes-Gutenberg University Mainz for taking videos of embryos, Dr. Christopher Michael Dooley from the Wellcome Trust Sanger Institute for providing the Nbt:DsRed line, Alexandra Lissouba Tatarinoff and Pierre Drapeau from the University of Montreal for discussions and help with Fus morpholino injections and Daniel Heylmann from the University Medical Center Mainz for the gamma-irradiation.

Funding

This work was supported by the core IMB funding.

Author Contributions

R.K. and S.L. designed the study, S.L. performed the wetlab experiments, A.D. and S.L. analyzed the data, F.B. performed mass-spectrometry and analyzed the MS data, S.L., A.D. and R.K. wrote the paper.

ORCID

António M. de Jesus Domingues http://orcid.org/0000-0002-1803-1863

References

1. Calabretta S, Richard S. Emerging Roles of Disordered Sequences in RNA-Binding Proteins. Trends Biochem Sci 2015; 40:662-72; PMID:26481498; http://dx.doi.org/10.1016/j.tibs.2015.08.012
2. Svetoni F, Frisone P, Paronetto MP. Role of FET proteins in neurodegenerative disorders. RNA Biol 2016; 13(11):1089-1102; PMID:27415968; http://dx.doi.org/10.1080/15476286.2016.1211225
3. Lagier-Tourenne C, Polymenidou M, Hutt KR, Vu AQ, Baughn M, Huelga SC, Clutario KM, Ling S-C, Liang TY, Mazur C, et al. Divergent roles of ALS-linked proteins FUS/TLS and TDP-43 intersect in processing long pre-mRNAs. Nat Neurosci 2012; 15:1488-97; PMID:23023293; http://dx.doi.org/10.1038/nn.3230
4. Ishigaki S, Masuda A, Fujioka Y, Iguchi Y, Katsuno M, Shibata A, Urano F, Sobue G, Ohno K. Position-dependent FUS-RNA interactions regulate alternative splicing events and transcriptions. Sci Rep 2012; 2:529; PMID:22829983; http://dx.doi.org/10.1038/srep00529
5. Rogelj B, Easton LE, Bogu GK, Stanton LW, Rot G, Curk T, Zupan B, Sugimoto Y, Modic M, Haberman N, et al. Widespread binding of FUS along nascent RNA regulates alternative splicing in the brain. Sci Rep 2012; 2:603; PMID:22934129; http://dx.doi.org/10.1038/srep00603
6. Reber S, Stettler J, Filosa G, Colombo M, Jutzi D, Silvia C, Schweingruber C, Bruggmann R, Bachi A, Barabino SML, et al. Minor intron splicing is regulated by FUS and affected by ALS-associated FUS mutants. 2016; 1-18.; PMID:27252488; http://dx.doi.org/10.15252/embj.201593791
7. Nakaya T, Alexiou P, Maragkakis M, Chang A. FUS regulates genes coding for RNA-binding proteins in neurons by binding to their highly conserved introns. RNA 2013; 19:498-509; PMID:23389473; http://dx.doi.org/10.1261/rna.037804.112
8. Masuda A, Takeda JI, Okuno T, Okamoto T, Ohkawara B, Ito M, Ishigaki S, Sobue G, Ohno K. Position-specific binding of FUS to nascent RNA regulates mRNA length. Genes Dev 2015; 29:1045-57; PMID:25995189; http://dx.doi.org/10.1101/gad.255737.114
9. Shelkovnikova TA, Robinson HK, Troakes C, Ninkina N, Buchman VL. Compromised paraspeckle formation as a pathogenic factor in FUSopathies. Hum Mol Genet 2014; 23:2298-312; PMID:24334610; http://dx.doi.org/10.1093/hmg/ddt622
10. Yamazaki T, Chen S, Yu Y, Yan B, Haertlein TC, Carrasco MA, Tapia JC, Zhai B, Das R, Lalancette-Hebert M, et al. FUS-SMN Protein Interactions Link the Motor Neuron Diseases ALS and SMA. Cell Rep 2012; 2:799-806; PMID:23022481; http://dx.doi.org/10.1016/j.celrep.2012.08.025
11. Kato M, Han TW, Xie S, Shi K, Du X, Wu LC, Mirzaei H, Goldsmith EJ, Longgood J, Pei J, et al. Cell-free formation of RNA granules: low complexity sequence domains form dynamic fibers within hydrogels. Cell 2012; 149:753-67; PMID:22579281; http://dx.doi.org/10.1016/j.cell.2012.04.017

12. Kwiatkowski TJ, Bosco D a, Leclerc AL, Tamrazian E, Vanderburg CR, Russ C, Davis A, Gilchrist J, Kasarskis EJ, Munsat T, et al. Mutations in the FUS/TLS gene on chromosome 16 cause familial amyotrophic lateral sclerosis. Science 2009; 323:1205-8; PMID:19251627; http://dx.doi.org/10.1126/science.1166066
13. Vance C, Rogelj B, Hortobágyi T, De Vos #2 KJ, Nishimura AL, Sreedharan J, Hu X, Smith B, Ruddy D, Wright P, et al. Mutations in FUS, an RNA Processing Protein, Cause Familial Amyotrophic Lateral Sclerosis Type 6. Science 2009; 323:1208-11; PMID:19251628; http://dx.doi.org/10.1126/science.1165942
14. Sharma A, Lyashchenko AK, Lu L, Nasrabady SE, Elmaleh M, Mendelsohn M, Nemes A, Tapia JC, Mentis GZ, Shneider NA. ALS-associated mutant FUS induces selective motor neuron degeneration through toxic gain of function. Nat Commun 2016; 7:10465; PMID:26842965; http://dx.doi.org/10.1038/ncomms10465
15. Scekic-zahirovic J, Sendscheid O, Oussini H El, Jambeau M, Ying S. Toxic gain of function from mutant FUS protein is crucial to trigger cell autonomous motor neuron loss. EMBO J 2016; 35:1077-97. PMID:26951610; http://dx.doi.org/10.15252/embj.201592559
16. Mitchell JC, McGoldrick P, Vance C, Hortobagyi T, Sreedharan J, Rogelj B, Tudor EL, Smith BN, Klasen C, Miller CCJ, et al. Overexpression of human wild-type FUS causes progressive motor neuron degeneration in an age- and dose-dependent fashion. Acta Neuropathol 2013; 125:273-88; PMID:22961620; http://dx.doi.org/10.1007/s00401-012-1043-z
17. Huang C, Zhou H, Tong J, Chen H, Liu YJ, Wang D, Wei X, Xia XG. FUS transgenic rats develop the phenotypes of amyotrophic lateral sclerosis and frontotemporal lobar degeneration. PLoS Genet 2011; 7 (3):e1002011; PMID:21408206; http://dx.doi.org/10.1371/journal.pgen.1002011
18. Kino Y, Washizu C, Kurosawa M, Yamada M, Miyazaki H, Akagi T, Hashikawa T, Doi H, Takumi T, Hicks GG, et al. FUS/TLS deficiency causes behavioral and pathological abnormalities distinct from amyotrophic lateral sclerosis. Acta Neuropathol Commun 2015; 3:24; PMID:25907258; http://dx.doi.org/10.1186/s40478-015-0202-6
19. Kuroda M, Sok J, Webb L, Baechtold H, Urano F, Yin Y, Chung P, de Rooij DG, Akhmedov A, Ashley T, et al. Male sterility and enhanced radiation sensitivity in TLS(−/−) mice. EMBO J 2000; 19:453-62; PMID:10654943; http://dx.doi.org/10.1093/emboj/19.3.453
20. Hicks GG, Singh N, Nashabi A, Mai S, Bozek G, Klewes L, Arapovic D, White EK, Koury MJ, Oltz EM, et al. Fus deficiency in mice results in defective B-lymphocyte development and activation, high levels of chromosomal instability and perinatal death. Nat Genet 2000; 24:175-9; PMID:10655065; http://dx.doi.org/10.1038/72842
21. Kabashi E, Bercier VV, Lissouba A, Liao M, Brustein E, Rouleau GA, Drapeau P. Fus and tardbp but not sod1 interact in genetic models of amyotrophic lateral sclerosis. PLoS Genet 2011; 7:e1002214; PMID:21829392; http://dx.doi.org/10.1371/journal.pgen.1002214
22. Armstrong GAB, Drapeau P. Loss and gain of FUS function impair neuromuscular synaptic transmission in a genetic model of ALS. Hum Mol Genet 2013; 22:4282-92; PMID:23771027; http://dx.doi.org/10.1093/hmg/ddt278
23. Blokhuis A, Koppers M, Groen E, Van DenHeuvel D, Modigliani SD, Anink J, Fumoto K, Diggelen F Van, Snelting A, Sodaar P, et al. Comparative interactomics analysis of different ALS-associated proteins identifies converging molecular pathways. Acta Neuropathol 2016; 132:175-96; PMID:27164932; http://dx.doi.org/10.1007/s00401-016-1575-8
24. Hwang WY, Fu Y, Reyon D, Maeder ML, Tsai SQ, Sander JD, Peterson RT, Yeh J-RJR, Joung JK. Efficient genome editing in zebrafish using a CRISPR-Cas system. Nat Biotechnol 2013; 31:227-9; PMID:23360964; http://dx.doi.org/10.1038/nbt.2501
25. Pasquier J, Cabau C, Nguyen T, Jouanno E, Severac D, Braasch I, Journot L, Pontarotti P, Klopp C, Postlethwait JH, et al. Gene evolution and gene expression after whole genome duplication in fish: the PhyloFish database. BMC Genomics 2016; 17:368; PMID:27189481; http://dx.doi.org/10.1186/s12864-016-2709-z
26. Monson C A, Sadler KC. Inbreeding depression and outbreeding depression are evident in wild-type zebrafish lines. Zebrafish 2010; 7:189-97; PMID:20438386; http://dx.doi.org/10.1089/zeb.2009.0648
27. Shenker S, Miura P, Sanfilippo P, Lai EC. IsoSCM: improved and alternative 3′ UTR annotation using multiple change-point inference. RNA 2015; 21:14-27; PMID:25406361; http://dx.doi.org/10.1261/rna.046037.114
28. Peri F, Nüsslein-Volhard C. Live Imaging of Neuronal Degradation by Microglia Reveals a Role for v0-ATPase a1 in Phagosomal Fusion In Vivo. Cell 2008; 133:916-27; PMID:18510934; http://dx.doi.org/10.1016/j.cell.2008.04.037
29. Granato M, van Eeden FJ, Schach U, Trowe T, Brand M, Furutani-Seiki M, Haffter P, Hammerschmidt M, Heisenberg CP, Jiang YJ, et al. Genes controlling and mediating locomotion behavior of the zebrafish embryo and larva. Development 1996; 123:399-413; PMID:9007258.
30. Frickenhaus M, Wagner M, Mallik M, Catinozzi M, Storkebaum E. Highly efficient cell-type-specific gene inactivation reveals a key function for the Drosophila FUS homolog cabeza in neurons. Sci Rep 2015; 5:9107; PMID:25772687; http://dx.doi.org/10.1038/srep09107
31. Kapeli K, Pratt GA, Vu AQ, Hutt KR, Martinez FJ, Sundararaman B, Batra R, Freese P, Lambert NJ, Huelga SC, et al. Distinct and shared functions of ALS-associated proteins TDP-43, FUS and TAF15 revealed by multisystem analyses. Nat Commun 2016; 7:12143; PMID:27378374; http://dx.doi.org/10.1038/ncomms12143
32. Schmid B, Hruscha A, Hogl S, Banzhaf-Strathmann J, Strecker K, van der Zee J, Teucke M, Eimer S, Hegermann J, Kittelmann M, et al. Loss of ALS-associated TDP-43 in zebrafish causes muscle degeneration, vascular dysfunction, and reduced motor neuron axon outgrowth. Proc Natl Acad Sci U S A 2013; 110:4986-91; PMID:23457265; http://dx.doi.org/10.1073/pnas.1218311110
33. Hoell JI, Larsson E, Runge S, Nusbaum JD, Farazi TA, Hafner M, Borkhardt A, Sander C, Tuschl T, Rockefeller T, et al. RNA targets of wild-type and mutant FET family proteins. Nat Struct Mol Biol 2011; 18:1428-31; PMID:22081015; http://dx.doi.org/10.1038/nsmb.2163
34. Sun S, Ling S, Qiu J, Albuquerque CP, Zhou Y, Tokunaga S, Li H, Qiu H, Bui A, Yeo GW, et al. ALS-causative mutations in FUS/TLS confer gain and loss of function by altered association with SMN and U1-snRNP. Nat Commun 2015; 6:6171; PMID:25625564; http://dx.doi.org/10.1038/ncomms7171
35. Kimmel CB, Ballard WW, Kimmel SR, Ullmann B, Schilling TF. Stages of embryonic development of the zebrafish. Dev Dyn 1995; 203:253-310; PMID:8589427; http://dx.doi.org/10.1002/aja.1002030302
36. Dobin A, Davis CA, Schlesinger F, Drenkow J, Zaleski C, Jha S, Batut P, Chaisson M, Gingeras TR. STAR: Ultrafast universal RNA-seq aligner. Bioinformatics 2013; 29:15-21; PMID:23104886; http://dx.doi.org/10.1093/bioinformatics/bts635
37. Liao Y, Smyth GK, Shi W. FeatureCounts: An efficient general purpose program for assigning sequence reads to genomic features. Bioinformatics 2014; 30:923-30; PMID:24227677; http://dx.doi.org/10.1093/bioinformatics/btt656
38. Love MI, Huber W, Anders S. Moderated estimation of fold change and dispersion for RNA-seq data with DESeq2. Genome Biol 2014; 15:550; PMID:25516281; http://dx.doi.org/10.1186/s13059-014-0550-8
39. Bluhm A, Casas-Vila N, Scheibe M, Butter F. Reader interactome of epigenetic histone marks in birds. Proteomics 2016; 16:427-36; PMID:26703087; http://dx.doi.org/10.1002/pmic.201500217
40. Cox J, Mann M. MaxQuant enables high peptide identification rates, individualized p.p.b.-range mass accuracies and proteome-wide protein quantification. Nat Biotechnol 2008; 26:1367-72; PMID:19029910; http://dx.doi.org/10.1038/nbt.1511
41. H. Wickham. ggplot2: Elegant Graphics for Data Analysis. Springer-Verlag New York; 2009.
42. Schindelin J, Arganda-Carreras I, Frise E, Kaynig V, Longair M, Pietzsch T, Preibisch S, Rueden C, Saalfeld S, Schmid B, et al. Fiji: an open source platform for biological image analysis. Nat Methods 2012; 9:676-82; PMID:22743772; http://dx.doi.org/10.1038/nmeth.2019
43. Cox J, Hein MY, Luber CA, Paron I, Nagaraj N, Mann M. Accurate proteome-wide label-free quantification by delayed normalization and maximal peptide ratio extraction, termed MaxLFQ. Mol Cell Proteomics 2014; 13:2513-26; PMID:24942700; http://dx.doi.org/10.1074/mcp.M113.031591